PREPARED FOR THE U.S. DEPARTMENT OF ENERGY,
UNDER CONTRACT DE-AC02-76-CHO-3073

PPPL-3091
UC-427

PPPL-3091

HIGH HARMONIC FAST WAVES IN HIGH BETA PLASMAS

BY

M. ONO

APRIL 1995

PRINCETON
PLASMA PHYSICS
LABORATORY

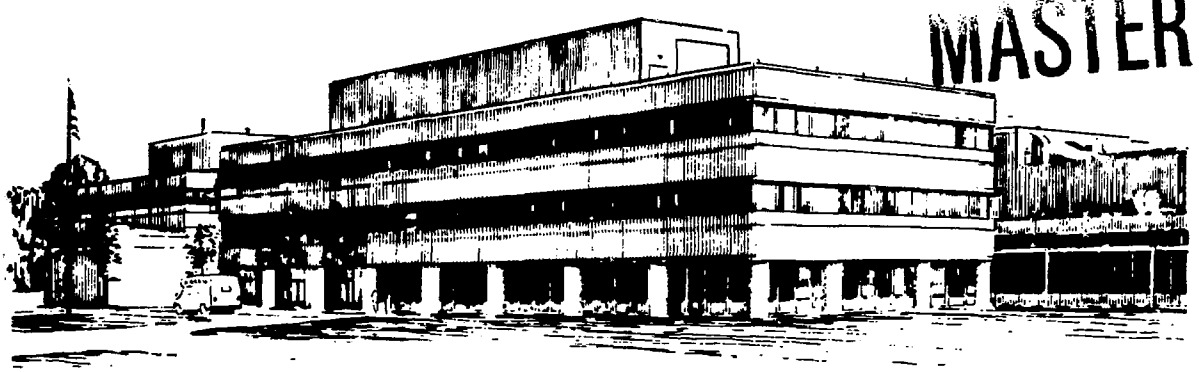

PRINCETON UNIVERSITY, PRINCETON, NEW JERSEY

NOTICE

NOTICE

High Harmonic Fast Waves in High Beta Plasmas

Masayuki Ono

Princeton Plasma Physics Laboratory, Princeton University
P.O. Box 451
Princeton, New Jersey 08543

Abstract

High harmonic fast magnetosonic wave in high beta / high dielectric plasmas is investigated including the finite-Larmor-radius effects. In this regime, due to the combination of group velocity slow down and the high beta enhancement, the electron absorption via electron Landau and electron magnetic pumping becomes significant enough that one can expect a strong (≈ 100%) single pass absorption. By controlling the wave spectrum, the prospect of some localized electron heating and current drive appears to be feasible in high beta low-aspect-ratio tokamak regimes. Inclusion of finite-Larmor-radius terms shows an accessibility limit in the high ion beta regime ($\beta_i \approx 50\%$ for a deuterium plasma) due to mode-conversion into an ion-Bernstein-wave-like mode while no beta limit is expected for electrons. With increasing ion beta, the ion damping can increase significantly particularly near the beta limits. The presence of energetic ion component expected during intense NBI and α-heating does not appear to modify the accessibility condition nor cause excessive wave absorption.

I. INTRODUCTION

Recently, low-aspect-ratio tokamaks (LART) have received considerable interest due to the encouraging small scale experimental results[1-3] as well as its promise for stable high beta tokamak regimes for the next generation LART experiments.[4] The reactor attractiveness of the LART regime has been also pointed out.[5] Indeed, some MHD stability calculations have shown stable high beta regimes with β in excess of 40% and high bootstrap current (pressure driven current) fraction of > 80%.[6] To heat and sustain such high beta plasmas by non-inductive means is an important topic for low-aspect-ratio tokamak research. A typical next generation high beta LART experimental regime has an unusually large plasma dielectric constant, $\varepsilon \equiv \omega_{pe}^2 / \Omega_e^2 \approx 100$. This compares with the conventional tokamak parameters of $\varepsilon \approx 1$. For the high dielectric plasmas, we find the accessibility of fast wave to the plasma core has a relatively low ion beta limit (typically $\beta_i \leq 10\%$) in the ion cyclotron range of frequency

$\omega \geq \Omega_i$ by the mode conversion to the ion Bernstein waves. For $\omega \leq \Omega_i$, the fast wave has a good wave accessibility but very weakly damped. It is also well known that in high dielectric regime, such waves as electron plasma waves (lower hybrid waves) and electron cyclotron waves have severe accessibility problems. On the other hand, the intermediate frequency range, i.e., $\Omega_i << \omega << \omega_{LH}$, appears to offer an attractive fast wave regime even in the high beta and high dielectric plasmas. In this work, we therefore limit the discussions on fast waves only to this intermediate wave frequency range.

The previous theoretical work for the fast waves in the intermediate range of frequency has been carried out in various regimes with dielectric constant typically $\varepsilon \approx 1$ in Refs. 7-11. The experimental evidence of direct fast wave current drive FWCD is relatively limited.[12-14] The direct electron heating has shown efficient central electron heating in several tokamak plasmas.[15-17] One of the limitations of FWCD is that since the power deposition is central, one can only drive the current in the central region owing to the relatively weak single pass power absorption in the low β experimental regimes. The present analysis shown here predicts sufficiently strong single pass absorption for high harmonic fast magnetosonic waves (HHFW) in this high dielectric regime that it may be possible to consider local power deposition and, therefore, current profile control by FWCD. Moreover, in this regime, the multi-megawatts radio frequency transmitters now being used for ICRF/IBW experiments can be utilized for electron heating/CD of the next generation LART devices where the confinement, MHD beta limits, and plasma sustainment can be explored. The plan of the present paper is as follows: In Sec. II, the general wave properties of high harmonic fast wave is discussed. In Sec. III, the wave damping due to electron magnetic pumping and electron Landau damping neglecting the ion-Larmor-radius effects is described. In this limit, one can show that the dispersion relation can be reduced to a quadratic form. One important result obtained here is that the magnetic pumping is dominant damping mechanism even though the frequency is high (ω being many time Ω_i). In Sec. IV, the effects of finite-ion-Larmor-radius are discussed. As the ion temperature is raised, the wavelength can approach the ion Larmor radius that the finite-Larmor-radius terms can no longer be neglected. In Sec. V, the profile effects are considered to estimate the single pass damping coefficients and the power deposition profiles. Finally, we present conclusions and discussions in Sec. VI.

II. HIGH HARMONIC FAST WAVE DISPERSION RELATION

In the high beta regime, the wave dielectric constant, ε is quite high for HHFW. This can be shown from the following simple analysis. We define $\beta_i \equiv 8\pi n_i \kappa T_i / B^2$ to be the ion beta and similarly β_e as the electron beta. Noting that $\beta_e \equiv 8\pi n_e \kappa T_e / B^2 = (\omega_{pe}^2/\Omega_e^2)(V_{Te}/c)^2$

$= \varepsilon (V_{Te}/c)^2$ one gets $\varepsilon = \beta_e (c / V_{Te})^2$ where $V_{Te} \equiv (2\,\kappa T_e/m_e)^{0.5}$. One can see that since $(c / V_{Te})^2$ is ≈ 100 for typical LART experimental parameters for $T_e \approx$ few keV, ε is order of 100 for plasmas with $\beta \approx 1.0$. For example, for typical central parameters for the NSTX target plasmas; $n_e \approx 5 \times 10^{13}$ cm^{-3} and $T_e \approx 1$ keV, and $B_T \approx 2.5$ kG in deuterium plasma, ε is 82 and electron beta is 34 %. We shall use these values as the nominal parameters for LART plasmas.

The HHFW dispersion relation is obtained from a non-trivial solution of the determinant of the wave equation tensor for Maxwellian plasmas as[18]

$$\det\begin{bmatrix} K_{xx} - n_{\parallel}^2 & -iK_{xy} & K_{xz} + n_{\perp} n_{\parallel} \\ K_{xy} & K_{yy} - n^2 & iK_{yz} \\ K_{xz} + n_{\perp} n_{\parallel} & -iK_{yz} & K_{zz} - n_{\perp}^2 \end{bmatrix} = 0 \qquad (1)$$

where

$$K_{xx} = 1 + \sum_{\sigma} \frac{\omega_{p\sigma}^2}{\omega} \sum_{n=-\infty}^{\infty} \frac{n^2 I_n(\lambda)\, e^{-\lambda}}{\lambda} \frac{1}{k_{\parallel} V_{T\sigma}} Z_0(y_n), \qquad (2\text{-a})$$

$$K_{xy} = \sum_{\sigma} \frac{\omega_{p\sigma}^2}{\omega} \sum_{n=-\infty}^{\infty} n \left(I_n - I_n'\right) e^{-\lambda} \frac{1}{k_{\parallel} V_{T\sigma}} Z_0(y_n), \qquad (2\text{-b})$$

$$K_{yy} = 1 + \sum_{\sigma} \frac{\omega_{p\sigma}^2}{\omega} \sum_{n=-\infty}^{\infty} \left(\frac{n^2}{\lambda} I_n + 2\lambda\, I_n - 2\lambda\, I_n' \right) \frac{e^{-\lambda}}{k_{\parallel} V_{T\sigma}} Z_0(y_n), \qquad (2\text{-c})$$

$$K_{xz} = -\sum_{\sigma} \frac{\omega_{p\sigma}^2}{\omega} \sum_{n=-\infty}^{\infty} e^{-\lambda} \frac{k_{\perp}}{\Omega} \frac{n I_n}{\lambda} \frac{1}{2k_{\parallel}} \frac{dZ_0(y_n)}{dy_n}, \qquad (2\text{-d})$$

$$K_{yz} = -\sum_{\sigma} \frac{\omega_{p\sigma}^2}{\omega} \sum_{n=-\infty}^{\infty} e^{-\lambda} \frac{k_{\perp}}{\Omega} (I_n - I_n') \frac{1}{2k_{\parallel}} \frac{dZ_0(y_n)}{dy_n}, \qquad (2\text{-f})$$

$$K_{zz} = 1 - \sum_{\sigma} \frac{\omega_{p\sigma}^2}{\omega} \sum_{n=-\infty}^{\infty} e^{-\lambda} \frac{2(\omega - n\Omega)}{k_{\parallel} V_{T\sigma}^2} I_n \frac{1}{2k_{\parallel}} \frac{dZ_0(y_n)}{dy_n}, \qquad (2\text{-g})$$

$y_n \equiv (\omega - n\Omega) / (k_{\parallel} V_{T\sigma})$, and $\lambda \equiv (k_{\perp}^2 \kappa T_i) / (\Omega_i^2 m_i) = (k_{\perp}\rho_i)^2/2$. I_n and I_n' are the n-th order modified Bessel function and its derivative, and Z_0 is the plasma dispersion function. The subscript σ is over all species.

III. ELECTRON ABSORPTION PROCESSES

For the present analysis, the wave frequency is high compared to the ion cyclotron frequency ($\omega \approx 21\ \Omega_D$), but well below the electron cyclotron frequency ($\omega \approx 0.006\ \Omega_e$). We also can neglect the FLR effects on electrons ($\lambda_e \equiv (m_e/m_i)\ \lambda_i \ll 1$). The terms which contribute to the electron damping are the $n = 0$ terms in K_{yy}, K_{yz}, K_{zy}, and K_{zz} elements of the dielectric tensor. For the present case, it is sufficient to keep the lowest order terms for λ_e. If we neglect the ion FLR terms, the dielectric elements are simplified to

$$K_{xxc} = 1 + \frac{\omega_{pe}^2}{\Omega_e^2} - \sum_i \frac{\omega_{pi}^2}{\omega^2 - \Omega_i^2}, \tag{3-a}$$

$$K_{xyc} = \frac{\omega_{pe}^2}{\omega\,\Omega_e} + \sum_i \frac{\omega_{pi}^2\,\Omega_i}{\omega(\omega^2 - \Omega_i^2)}, \tag{3-b}$$

$$K_{yyc} = K_{xxc} + n_\perp^2 \frac{\omega_{pe}^2}{\Omega_e^2}\frac{V_{Te}^2}{c^2}\frac{\omega}{k_\parallel V_{Te}} Z_0(y_0) = K_{xxc} + n_\perp^2\,\delta_m\,, \tag{3-c}$$

$$K_{xzc} = -n_\perp n_\parallel \sum_i \frac{\omega_{pi}^2\,\omega^2\,V_{Ti}^2}{c^2(\omega^2 - \Omega_i^2)^2} = n_\perp n_\parallel\,\delta, \tag{3-d}$$

$$K_{yz} \cong -n_\perp \frac{V_{Te}^2\,k_\parallel}{2c\Omega_e} K_{zze} = -n_\perp \delta_x K_{zze}, \text{ and} \tag{3-e}$$

$$K_{zz} \cong 1 - \sum_i \frac{\omega_{pi}^2}{\omega^2} - \frac{\omega_{pe}^2}{k_\parallel^2 V_{Te}^2}\frac{dZ_0(y_0)}{dy_0} \cong -\frac{\omega_{pe}^2}{k_\parallel^2 V_{Te}^2}\frac{dZ_0(y_0)}{dy_0} = K_{zze} \tag{3-f}$$

where δ_m is the magnetic pumping (MP) term and K_{zze} gives the electron Landau damping (ELD). δ_x represents the cross (X) terms in K_{yz}. For cold ions, δ in K_{xz} though being kept here is actually very small (< 0.01). In the high beta regime, usually δ_x is small, but δ_m is of order unity. One can then rewrite the determinant in Eq. (1) in the following simple form,

$$\det\begin{bmatrix} K_{xxc} - n_\parallel^2 & -iK_{xyc} & n_\perp n_\parallel(1+\delta) \\ iK_{xyc} & K_{xxc} - n_\parallel^2 - n_\perp^2(1-\delta_m) & -in_\perp\delta_x K_{zz} \\ n_\perp n_\parallel(1+\delta) & in_\perp\delta_x K_{zz} & K_{zz} - n_\perp^2 \end{bmatrix} = 0. \tag{4}$$

The above determinant is convenient for solving for $n_\perp$ for a given ω and $n_\parallel$ since all K's and δ's are independent of $n_\perp$. Indeed, one can readily solve for $n_\perp$ by noting that the determinant takes on the following quadratic form in $n_\perp^2$:

$$a\, n_\perp^4 + b\, n_\perp^2 + c \;=\; 0 \qquad (5)$$

where

$$a \;=\; [(n_\parallel^2 - K_{xxc}) - n_\parallel^2\,(1+\delta)^2\,]\,(1-\delta_m\,),$$

$$b \;=\; -K_{xy}^2 - \delta_x^2(n_\parallel^2 - K_{xxc})\,K_{zze}^2 - (n_\parallel^2 - K_{xxc})(1-\delta_m\,)\,K_{zze}$$
$$+\,2\,\delta_x n_\parallel\,(1+\delta)K_{zze}\,K_{xyc} + (n_\parallel^2 - K_{xxc})^2 - n_\parallel^2\,(1+\delta)^2(n_\parallel^2 - K_{xxc})$$

, and

$$c \;=\; \left[K_{xyc}^2 - (n_\parallel^2 - K_{xxc})^2\right] K_{zze}.$$

The subscripts "c" and "e" denote cold ions and kinetic electrons. To see the magnitude of various damping terms, we show in Fig. 1 some numerical examples. The parameters are n_e = 5 x 10^{13} cm^{-3}, T_e = 2 keV, B = 2.5 kG, pure deuterium plasma, and the rf frequency of 41 MHz. This corresponds to about 21 - 22 harmonics of deuterium ion cyclotron frequency. In Fig. 1a, the real part of the perpendicular wave number $k_{\perp r}$ is plotted as a function of $n_{\parallel}$. Here, for $n_{\parallel}$ = 8, the wave parallel phase velocity is twice the electron thermal velocity, i.e., $\omega/k_{\parallel} = 2\,V_{Te}$. To illustrate the contributions of each terms, four cases are shown in the figure: rhombuses = ELD + X terms; squares = ELD only; crosses = ELD + X terms; and circles = all terms (ELD + MP + X) being included. The expected perpendicular wave number (noting that $\omega/k_\perp = V_{ph\perp} \approx V_A$), $k_\perp \approx \omega/V_A \equiv \omega\,(\omega_{pi}/\,c\,\Omega_i\,) \propto n^{0.5}\,/\,B$, is 4.745 as indicated in the figure. This value agrees relatively well with the calculated wave number without MP. As can be seen from the figure, the inclusion of the MP term causes about 15 % down shift in the wave number. The MP contribution is quite significant in the damping term. In Fig. 1(b) the corresponding imaginary part of the perpendicular wave number is shown. As can be seen from the figure, the inclusion of MP term (crosses) drastically increase the damping over the ELD alone case (squares). In this high beta regime, even though the frequency is relatively high, the magnetic pumping is very important. The X terms (rhombuses) actually reduces the damping (giving fictitious negative damping). The case with ELD+MP+ X terms (circles), still shows a considerable damping enhancement, i.e., three to four times the ELD only case. The electron damping becomes significant for $n_{\parallel}$ larger than 6 or $\omega/k_{\parallel} \le 2.5\,V_{Te}$. Indeed for $n_{\parallel}$ = 10, the expected power damping length, $L_D \approx (2\,Im\,k_\perp)^{-1}$ becomes less than 10 cm which indicates a complete single pass absorption.

The dependence of damping on the density and magnetic field is also instructive. In Fig. 2, we show the behavior of the wave number as a function of magnetic field. The wave number varies inversely with the magnetic field as shown in Fig. 2(a). This is consistent with $k_\perp \approx \omega/V_A \equiv \omega\,(\omega_{pi}/\,c\,\Omega_i\,) \propto n^{0.5}\,/\,B$. The damping shows an even more strong dependence of B^{-3} as shown in Fig. 2(b). This is consistent with the previous results (Ref. 6-9) that the fast wave damping is proportional to the plasma beta times the wave number. However, a curious observation is that the damping is not nearly as strongly dependent on the plasma density. In Fig. 3, we show the density dependence of the wave number. The wave number goes up as the square root of the plasma density as expected from the Alfven velocity behavior as in Fig. 3(a). If Fig. 3(b), the damping is plotted as a function of the density. The dependence is at most linear with the density. Since for a fixed temperature, the plasma beta goes up linearly with the density, one would expect the damping to increase as $n_e^{1.5}$. Therefore, the damping picture in this high beta regime is not simply the wave number times the plasma beta for the density case. This behavior might be due to the delicate but different dependences of dielectric tensor elements with B and n_e. For example, $K_{xy} \propto B^{-1}$ but K_{xx} is nearly constant with B while both K_{xy} and K_{yy} increases linearly with the density.

IV. FINITE-ION-LARMOR-RADIUS EFFECTS

A. Accessibility Limit due to Ion Beta

As the ion temperature is increased, the finite-Larmor-radius effects become important in the high beta regime. If the ion beta is high, then the wave phase and group velocities approach the ion thermal velocities, noting that $\beta_i \equiv 8\,\pi\,n_i\,\kappa T_i\,/B^2 = (\omega_{pi}^2/\Omega_i^2)\,(V_{Ti}/c)^2 = (V_{Ti}/V_A)^2$ where $V_A \equiv B\,/\,(4\pi n_i m_i)^{0.5}$ and since $V_p \approx V_A$, one can see that V_{Ti} approaches V_A as $\beta \Rightarrow 1$. For the LART parameters of T_i = 1 keV and $n_i = 5 \times 10^{13}$ cm^{-3}, $\beta_i \approx 34$ %, $V_A \approx 1.7\,V_{Ti}$. In this regime, the FLR effects are becoming important. One can also rewrite that $\beta_i \equiv 8\,\pi\,n_i\,\kappa T_i\,/B^2 = (\omega_{pi}^2/\Omega_i^2)\,(V_{Ti}/c)^2 \approx 2\,(\,\Omega_i\,/\,\omega)^2\,\lambda$ or $\lambda \approx 0.5\,(\omega\,/\,\Omega_i\,)^2\beta_i$. Letting $\omega \approx n\,\Omega_i$, $\lambda \approx 0.5\,n^2\beta_i$ or $\lambda \approx n^2\,/\,6$ for the NSTX. Since the function $f(\lambda) = \lambda\,I_n\,e^{-\lambda}$ assumes the maximum value at $\lambda = n^2\,/\,3$, the λ parameter is getting quite large. In Fig. 4, the effect of FLR on the FW dispersion relation is shown. The full kinetic dispersion relation in Eq. (1) is solved where the sufficient number of FLR terms are included typically up to n = 50. The plasma parameters in Fig. 4 (a) are the same as shown in the previous cases [$n_e = n_D = 5 \times 10^{13}$ cm^{-3}, T_e = 1 keV, B = 2.5 kG, $n_{//}$ =8.]. As shown in Fig. 4(a), the real and imaginary parts of the wave number do not vary very much with ion temperature even though the λ factor is getting large which is somewhat surprising. The real part of dispersion relation hardly

changes while the imaginary part decreases only by 30% before going back up to near the cold ion value. Therefore, it appears as though the cold ion approximation is reasonably good here. However, as the ion temperature approaches 1500 eV in Fig. 4(a), the dispersion relation fails to converge quite abruptly. A detailed examination of the behavior shows that the group velocity goes to zero at that point indicating a mode conversion into an IBW-like-backward wave due to the FLR-effects. As mentioned earlier, this mode conversion process tends to occur for lower ion beta as the harmonic number is reduced. This means that the access to the finite ion beta plasma is limited by this FLR-mode-conversion process. Though this presents an actual limit to the fast wave accessibility, this ion beta limit is still over 50 % which is quite large. In Fig. 4(b), the magnetic field is raised to 3.45 kG (an increase of about 40%) in otherwise identical plasma. The temperature limit nearly doubles which is consistent with the same beta limit of 50 %. If the fast wave is used to heat or drive current in the off-axis region, for example, then the beta limit in the wave accessibility probably would not limit the wave performance.

B. Ion Cyclotron Harmonic Damping

As the wave moves through the plasmas with varying magnetic field, it is expected to cross ion cyclotron harmonic resonances Assuming the plasma to be magnetized, the resonance occurs at $\omega = n\Omega_i$. For 2.5 kG, 41 MHz case, n is about 21 for deuterium. The damping terms are from the imaginary part of the Z-function in K_{xx} and K_{xy}. Assuming small absorption, one can estimate the imaginary part of $k_\perp$ as,

$$\mathrm{Im}\, k_\perp = -\,\mathrm{Im}\, K_{xx}\,\frac{\partial D(K_{xx},K_{xy})/\partial K_{xx}}{\partial D/\partial k_\perp} - \mathrm{Im}\, K_{xy}\,\frac{\partial D(K_{xx},K_{xy})/\partial K_{xy}}{\partial D/\partial k_\perp}, \tag{6}$$

where

$$\mathrm{Im}\, K_{xx} = \sum_i \frac{\omega_{pi}^2}{\omega} \sum_{n=-\infty}^{\infty} \frac{n^2\, I_n(\lambda)\, e^{-\lambda}}{\lambda} \frac{\sqrt{\pi}}{k_\parallel V_{Ti}} \cdot \exp\left[-\left(\frac{\omega - n\Omega_i}{k_\parallel V_{Ti}}\right)^2\right],$$

$$\mathrm{Im}\, K_{xy} = \sum_i \frac{\omega_{pi}^2}{\omega} \sum_{n=-\infty}^{\infty} n\, (I_n - I_n')\, e^{-\lambda} \frac{\sqrt{\pi}}{k_\parallel V_{T\sigma}} \cdot \exp\left[-\left(\frac{\omega - n\Omega_i}{k_\parallel V_{Ti}}\right)^2\right],$$

and D is the determinant of the matrix in Eq. (1). The total fractional absorption factor across the n-th harmonic resonance of ion species i, $\Gamma_{i,n} = 2\int \mathrm{Im}\, k_\perp\, dx$ is obtained by integrating

through the resonance assuming the real part of the dispersion relation is not strongly affected. We then obtain

$$\Gamma_{i,n} = \frac{2k_\perp R\pi}{\left|k_\perp \partial D/\partial k_\perp\right|}\left[\frac{\omega_{pi}^2}{\Omega_i^2}\frac{I_n e^{-\lambda}}{\lambda}\cdot\frac{\partial D}{\partial K_{xx}} + \frac{\omega_{pi}^2}{\omega\Omega_i}\left(I_n - I_n'\right)e^{-\lambda}\cdot\frac{\partial D}{\partial K_{xy}}\right]. \quad (8)$$

The R represents a characteristic length of the magnetic field variation. In Fig. 5(a), Γ_D due to a deuterium resonance is plotted as a function of T_i for various plasma density for B = 2.5 kG and R = 80 cm. As shown in the figure, the damping is negligible until the ion temperature reaches a certain value. Reducing the density allows higher ion temperature, roughly preserving a constant beta dependence. This constant β condition is equivalent to constant $\lambda \equiv (1/2)(k_\perp\rho_i)^2$. One should also note that this heavy ion harmonic damping occurs when $\omega/k_\perp$ approaches near $2xV_{Ti}$. This is consistent with the unmagnetized model where the perpendicular ion Landau damping increases as $\omega/k_\perp$ approaches ≈ 2-3 V_{Ti}. The observed constant beta condition also agrees with the $\omega/k_\perp \propto (n_e)^{-0.5} \propto V_{Ti}$ dependence. It is interesting that the magnetized model and unmagnetized model both predict similar damping trends in this high harmonic cyclotron frequency regime. In Fig. 5(b), we show the damping dependence of the magnetic field. Again by increasing the magnetic field by 40 %, we see the temperature limit increase by a factor of two in accordance with the constant ion beta condition. The damping due to non-hydrogenic impurity ions are negligible due to heavier mass (smaller ρ_i) resulting in smaller values of λ. However, the presence of excessive hydrogen ions would cause significant absorption due to its light mass. Typically hydrogen ions can cause two orders of magnitude larger absorption as deuterium ions. It is, therefore, important to keep the hydrogen to a low value ≤ few % which is possible by minimizing the hydrogen contamination into the vacuum system. If the hydrogen concentration can be kept low, then the quasi-linear effect is expected to further reduce the absorption by flattening the hydrogen distribution function.

C. Effects of Hot Ion Component

The behavior of increased ion damping with increased ion temperature raises the question of possible effects due to hot ion component expected, for example, during an intense NBI (neutral beam injection) heating and/or Alpha-particle heating.[20,21] To semi-qualitatively assess the damping due to hot ions, we modeled the hot ion component as 5% deuterium ions having some characteristic ion temperature, T_{hot}. One can, of course, extend the present result with other concentration values reasonably well by simply scaling the damping values from the present 5% value. In Fig. 6, we plot the damping behavior as T_{hot} is varied. The parameters

are $T_e = T_{bulk} =$ 1 keV, $n_{//} = 8$, $B \simeq 2.5$ kG, and $n_e = n_D = 3 \times 10^{13}$ cm^{-3}. As shown in Fig. 6(a), the effect of hot ion component on the real and imaginary (electron damping) parts of the wave number is quite negligible. The presence of hot ions also does not change the behavior of bulk ion absorption significantly. One interesting finding here is that the absorption by the hot ion component does not necessarily keep getting worse as its effective temperature is raised. In fact, after reaching the maximum value of 15 % around 10 keV, the absorption decreases rapidly with something like $T_{hot}^{-3/2}$. This is due to the behavior of the function $f(\lambda) = \lambda I_n e^{-\lambda}$ which reached maximum value at $\lambda = n^2/3$ (see for example, Chap. 11 of Ref. 9). Further increase in λ causes the damping term to decrease. Since for large λ, $f(\lambda) = \lambda^{-3/2}$, one can explain the drop in Γ_{hot} as $T_{hot}^{-3/2}$. This behavior is similar to that of the ion Bernstein waves where because of the short wave length, the damping due to hot ion components can be small. From the unmagnetized point of view, it is well known that the damping decreases as the wave phase velocity decreases to well below the hot ion velocity, i.e., $\omega/k_\perp << V_{hot}$. To properly assess the damping due to the hot species, it is necessary to use the non-Maxwellian distribution functions. For α–particles, the distribution function $F_\alpha(v)$ can be shown to be proportional to $1/(v^3 + v_c^3)$ where v_c is the critical velocity.[21] The damping which is proportional to the derivative of the distribution function is then $\partial F_\alpha(v)\partial v \propto - v^2 / (v^3 + v_c^3)^2$ goes down below the critical velocity as $\approx - v^2 / v_c^6$. Nevertheless, the actual distribution function may be more complicated in this lower velocity range and, thus, would require more careful examination.

V. PLASMA PROFILE EFFECTS

One can obtain a little more qualitative picture of the HHFW absorption by using typical plasma profiles. Here for simplicity, we assume the Gaussian profiles for the density and temperatures. In Fig. 7(a), the real and imaginary $k_\perp$ calculated using Eq. (5) as the function of the major radius is plotted for $n_{//} = 7$ where $n_0 = 5 \times 10^{13}$ cm^{-3}, $T_{e0} = 1$ keV, $R_0 = 80$ cm and $B_0 = 2.5$ kG. In Fig. 7(b) the normalized power and the power absorption profiles are shown. The wave is assumed to be launched from the outside radial position. One can see that the absorption is central and the single pass absorption is quite significant, $\approx$ 50%. The absorption can be increased by increasing $n_{||}$ as can be seen from Fig. 1. As the single pass absorption increases to near 100%, the absorption layer moves toward outside. The absorption also increases with electron temperature for given $n_{//}$. In Figs. 8 & 9, the central electron temperature of 3 keV is shown for $n_{//} = 4$ and 5, respectively. For $n_{//} = 4$ case, the heating is central with 50% absorption while $n_{//} = 5$ case, the heating moves toward off-axis. Increasing $n_{//}$ further would move the deposition layer further toward the plasma edge. Therefore, by

changing $n_{//}$ for a given electron temperature profile, one would have some control over the power deposition profile. The strong local absorption with relatively low $n_{//}$ values suggests a possibility of efficient local current drive which is useful for current profile control.

VI. CONCLUSIONS AND DISCUSSIONS

High harmonic fast wave appears to offer a promising tool for heating high beta LART plasmas. In this high beta regime, the magnetic pumping significantly increases the damping over the electron Landau damping alone. In Sec. III, the damping is found to scale as $k_{\perp i} \propto n_e / B^3$ and it is found to become significant for $\omega/k_{//} \leq 2.5\ V_{Te}$. This condition is almost like that of electron plasma wave (where the damping condition is known to be $\omega/k_{//} \leq 3\ V_{Te}$.) as opposed to the usual fast wave heating regime which requires $\omega/k_{//} \approx V_{Te}$ for any significant absorption. The strong damping offers the possibility of localized absorption which is needed for current profile control by current drive.[22] Heating of electrons enhances the current drive efficiency which goes up with $n_{//}^{-2} \propto T_e$. Based on the previous current drive scaling and strong local absorption for $\omega/k_{//} \approx 2.0\ V_{Te}$, one can expect the current drive efficiency for the fast wave in this regime to be,

$$I_{CD}(MA) \cong \frac{6\, P_{rf}(MW)}{n_e\,(10^{13} cm^{-3})\, R(m)\, n_{//}^2} \cong \frac{0.08\, P_{rf}(MW)\, T_e(keV)}{n_e\,(10^{13} cm^{-3})\, R(m)}.$$

One should point out that the previous analysis showed that the electron trapping effects reduces the current drive efficiency as the radial position is increased, typically by half at the half radius region.[8] This condition together with the decreasing temperature (though the decreasing density may help offset this trend) tends to make the rf-based current drive near the plasma periphery not practical. The higher electron temperature also increases the bootstrap and other forms of pressure driven currents through higher electron pressure and lower collisionality.

Analyses including ion-Larmor-radius effects indicate that while there is no practical electron beta limit, there is a limit for the ion beta. The wave accessibility is limited due to the mode conversion into an ion-Bernstein-wave-like mode. However the ion beta limit is around 50 % which is quite high. Perhaps more stringent condition is imposed due to the ion cyclotron harmonic absorption. The condition for significant deuterium cyclotron resonance absorption is similar to the perpendicular ion Landau damping in the unmagnetized model, $\omega/k_{\perp} \leq 2.0\ V_{Ti}$. The ion absorption condition lowers the ion beta limit toward 30%. While

this value is still acceptable, it is important to limit the ion beta if fast wave is used to heat plasmas toward the expected beta limit. For example, as long as the electron beta is larger than the ion beta (say 2:1), there is no problem until the total plasma beta is 90%. The effects of hot ions are also investigated in Sec. IV-B. The result shows that the presence of hot ions does not appear to cause excessive absorption. After reaching the maximum absorption values near 10 keV, the absorption again decreases for higher hot component temperature. At very high temperature, the damping decreases as $T_{hot}^{-3/2}$. This type of analysis indicates that HHFW can still be effective with NBI heating and/or the Alpha heating which is an encouraging result. However, since the velocity distribution of hot ion species are typically not Maxwellian, it would be necessary to use more precise velocity distribution functions which depend strongly on the actual circumstances. The slowness of the HHFW might also make it a good candidate for the use in Alpha-channeling in this high beta regime.[23]

In order to maximize electron heating, it is important to minimize the ion damping. While non-hydrogenic impurity absorption is negligible, the presence of hydrogen can lead to a significant absorption due to the faster speed and lower harmonic number (half the deuterium). It is very important to limit the hydrogen concentration to a few percent. This should not be too difficult by limiting the source of possible hydrogen contamination. While the prospect of fast wave heating and current drive in high beta low-aspect-ratio tokamak plasmas is good, it is important to carry out more detailed wave calculations using more precise tokamak geometry. Due to the short perpendicular wavelength nature of HHFW in high beta regime (typically 1 - 2 cm which is much less than the system size), the ray-tracing technique should be applicable to investigate this problem.

ACKNOWLEDGMENTS

This work was supported by U.S. Department of Energy contract No. DE-AC02-76-CHO-3073. The author acknowledges helpful discussions and suggestions from R. Goldston, S. Kaye, D. Ignat, R. Majeski, W. Nevins, M. Porkolab, T.H. Stix and J.R. Wilson. Special thanks are due to J. Menard for independently checking the calculations carried out in the manuscript.

REFERENCES

[1] Y. S. Hwang, M. Yamada, T. G. Jones, M. Ono, W. Choe, S. Jardin, E. Lo, G. Ludwig, J. Menard, A. Fredriksen, R. Nazikian, N. Pomphrey, S. Yoshikawa, A. Morita, Y. Ono, T. Itagaki, M. Katsurai, and K. Tokimatsu, in <Proceedings of the Fifteenth International Conference on Plasma Physics and Controlled Nuclear Fusion Research>, (Seville, Spain, September 1994) (International Atomic Energy Agency, Vienna, Austria) IAEA -CN-60/A5-II-6-2.

[2] T. R. Jarboe, B.A. Nelson, D.J. Orvis, L.A. McCullough, J. Xie, C. Zhang, and L. Zhou, in <Proceedings of the Fifteenth International Conference on Plasma Physics and Controlled Nuclear Fusion Research>, (Seville, Spain, September 1994) (International Atomic Energy Agency, Vienna, Austria)IAEA -CN-60/A5-II-6-1.

[3] A. Sykes, R.J. Colchin, R. Duck, S.K. Erents, D.H.J. Goodall, M. Gryaznevich, J. Hugill, I. Jenkins, R. Martins, A.R. Polevoic, C. Ribeiro, M. F. Turner, M. J. Walshj, and H.R. Wilson, in <Proceedings of the Fifteenth International Conference on Plasma Physics and Controlled Nuclear Fusion Research>, (Seville, Spain, September 1994) (International Atomic Energy Agency, Vienna, Austria), IAEA-CN-60/A5-II-5.

[4] See for example the Summary Report on the CST Workshop, July 1994, Oak Ridge, edited by Y. -K. M. Peng

[5] Y-K. M. Peng, R. J. Colchin, C. L. Hedrick, J. D. Galambos, J. Sheffield, D.J. Strickler, R. A. Blanken, A. Sykes, D. C. Robinson, A. W. Morris, J.Hugill, T. C. Hender, K. Erents, and H. R. Wilson, in <Proceedings of the Fifteenth International Conference on Plasma Physics and Controlled Nuclear Fusion Research>, (Seville, Spain, September 1994) (International Atomic Energy Agency, Vienna, Austria) IAEA -CN-60/F-I-3-2.

[6] S. Kaye, R.J. Goldston, Y.S. Hwang, S. Jardin, R. Kaita, J. Menard, and M. Ono, U.S./Japan Workshop on the Physics of Steady-State Tokamaks, LLNL, Calif. (Feb. 1995).

[7] T.H. Stix, Nucl. Fusion 15, 737 (1975).

[8] D.A. Ehst, K. Evans, Jr., D.W. Ignat, Nucl. Fusion 26, 461 (1986).

[9] D. Moreau, M.R. O'Brien, M. Cos, and D.F.H. Start, in Proceedings of the 14th European Conference on Controlled Fusion and Plasma Physics, (Madrid, 1987) 11D, Part III, (EPS, 1987) p. 1007.

[10] S. C. Chiu, V.S. Chan, R.W. Harvey, and M. Porkolab, Nucl. Fusion 29, 2175 (1989).

[11] M. Porkolab, Radio-Frequency Power in Plasmas: Ninth Topical Conference, Charleston, SC 1992 (American Institute of Physics, New York, 1992), p. 197.

[12] J. Goree, M. Ono, P. Colestock, D. McNeill, and H. Park, Phys. Rev. Lett. 55, 1669 (1985).

[13] R. Ando, E. Kako, Y. Ogawa, and T. Watari, Nucl. Fusion 26, 1619 (1986).
[14] R.I. Pinsker, C.C. Petty, M. Porkolab, F.W. Baity, P.T. Bonoli, R.W. Callis, W.P. Cary, S.C. Chiu, R.L. Freeman, R.H. Goulding, J.S. Degrassie, R.W. Harvey, D.J. Hoffman, R.A. James, H. Kawashima, T.C. Luce, M.J. Mayberry, R. Prater, and the DIII-D Team, in <Proceedings of the Fourteenth International Conference on Plasma Physics and Controlled Nuclear Fusion Research>, (Wurtzburg, Germany, September 1992) (International Atomic Energy Agency, Vienna, Austria) Paper IAEA -CN-56/E-2-4.
[15] T. Yamamoto, Y. Uesugi, H. Kawashima, K. Hoshino, H. Aikawa, S. Kasai, T. Kawakami, T. Kondoh, H. Maeda, T. Matsuda, H. Matsumoto, Y. Miura, M. Mori, K. Odajima, H. Ogawa, T. Ogawa, K. Ohasa, H. Ohtsuka, S. Sengoku, T. Shoji, N. Suzuki, H. Tamai, T. Yamauchi, and I. Nakazawa, Phys. Rev. Lett. 63, 1148 (1989).
[16] C.C. Petty, R. I. Pinsker, M.J. Mayberry, M. Porkolab, F.W. Baity, P.T. Bonoli, S.C. Chiu, J.C. M. de Haas, R.H. Goulding, D.J. Hoffman, T.C. Luce, and R. Prater, Phys. Rev. Lett. 69, 289 (1992).
[17] B. Saoutic and Equipe Tore Supra Team, in <Proceedings of the Fifteenth International Conference on Plasma Physics and Controlled Nuclear Fusion Research>, (Seville, Spain, September 1994) (International Atomic Energy Agency, Vienna, Austria) Paper IAEA -CN-56/A-3-I-6.
[18] T.H. Stix, Waves in Plasmas (American Institute of Physics, New York 1992).
[19] For a review of IBW and FLR-effects, see for example, Ono, Phys. Fluids B 5, 241 (1993).
[20] K.L. Wong and M. Ono, Nucl. Fusion 24, 615 (1984).
[21] A. Fukuyama, S.I. Itoh, K. Itoh, and K. Hamamatsu, ITER Report, Report # ITER-IL-Ph-6-9-J-6.
[22] N. J. Fisch, Review of Modern Physics 59, 175 (1987).
[23] N. J. Fisch and J.M. Rax, Phys. Rev. Lett. 69, 612 (1992).

Figure Captions

Fig. 1. HHFW perpendicular wave number as a function of $n_{//}$. $n_e = 5 \times 10^{13}$ cm^{-3}, $T_e = 1$ keV, $B = 2.5$ kG, $f = 41$ MHz, and deuterium plasma. (a) Real part of the wave number as a function of $n_{//}$ with various combination of damping terms, as labeled. (b) Corresponding imaginary part of the wave number as a function of $n_{//}$.

Fig. 2. Perpendicular wave number as a function of magnetic field for $n_{//} = 8$ and 12. $n_e = 5 \times 10^{13}$cm^{-3}, $T_e = 1$ keV, $f = 41$ MHz, and deuterium plasma. (a) Real part of the wave number as a function of magnetic field. $n_{//}$ as labeled. (b) Corresponding imaginary part of the wave number.

Fig. 3. Perpendicular wave number as a function of plasma density for $n_{//} = 8$ and 12. $T_e = 1$ keV, $B = 2.5$ kG, $f = 41$ MHz, and deuterium plasma. (a) Real part of the wave number as a function of plasma density. $n_{//}$ as labeled. (b) Corresponding imaginary part of the wave number.

Fig. 4. Perpendicular wave number as a function of ion temperature. $n_{//} = 8$, $n_e = 5 \times 10^{13}$cm^{-3}, $T_e = 1$ keV, $f = 41$ MHz, and deuterium plasma. (a) Real and imaginary parts of the wave number as a function of ion temperature for $B = 2.5$ kG. (b) Similarly for $B = 3.45$ kG.

Fig. 5. Fractional wave power absorption across the deuterium ion cyclotron harmonic frequency Γ_D as a function of ion temperature. $n_{//} = 8$, $T_e = 1$ keV, $n = 21$, and deuterium plasma. (a) Γ_D as a function ion temperature for various plasma density as labeled. $B \approx 2.5$ kG and $f = 41$ MHz.. (b) Γ_D as a function ion temperature for $B \approx 2.5$ and 3.47 kG, $f = 57$ MHz, and $n_e = 3 \times 10^{13}$cm^{-3}.

Fig. 6. Effects of hot ion component. $N_{hot} = 5$ %. $T_e = 1$ keV, $n_e = 3 \times 10^{13}$cm^{-3}, $f = 41$ MHz, $B \approx 2.5$ kG, $n = 21$, $n_{||} = 8$, and deuterium plasma. (a) Real and imaginary parts of perpendicular wave number (due to electron damping) as a function of hot component temperature. (b) Fractional wave power absorption across the deuterium ion cyclotron harmonic frequency as a function of hot component temperature. Γ_{bulk} denotes damping by the bulk deuterium and Γ_{hot} by the hot deuterium component.

Fig. 7. Profile effects in a typical NSTX regime. $R_0 = 80$ cm, $a = 64$ cm, $T_{e0} = 1$ keV, $n_{e0} = 5 \times 10^{13}$ cm^{-3}, $f = 41$ MHz, $B_0 = 2.5$ kG, and $n_{//} = 7$. Density and temperature profiles are Gaussian. $q(0) = 1$ and $q(a) = 3.5$. (a) Real and imaginary parts of the perpendicular wave number as a function of major radius. (b) Fractional power and absorbed power (arb. unit) as a function of major radius. Wave is assumed to be launched at $R = 144$ cm.

Fig. 8. Profile effects as in Fig. 7 with $T_{e0} = 3$ keV and $n_{//} = 4$.

Fig. 9. Profile effects as in Fig. 7 with $T_{e0} = 3$ keV and $n_{//} = 5$.

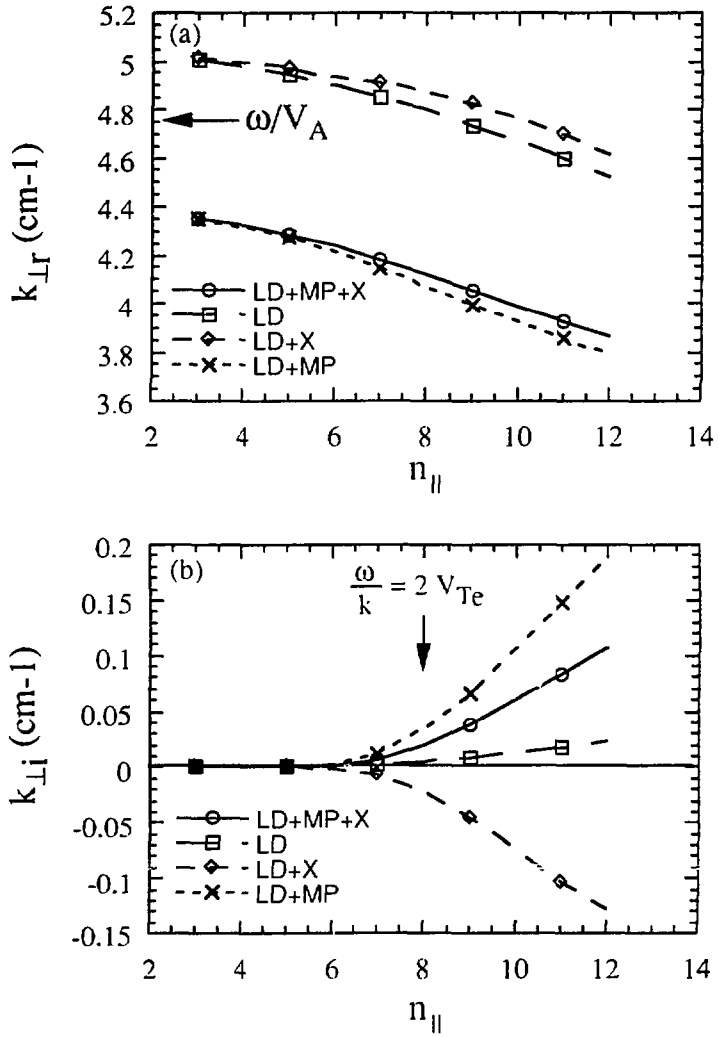
(a)
ω/V_A
LD+MP+X
LD
LD+X
LD+MP
k⊥r (cm-1)
n||
(b)
ω/k = 2 V_Te
LD+MP+X
LD
LD+X
LD+MP
k⊥i (cm-1)
n||

Fig. 1

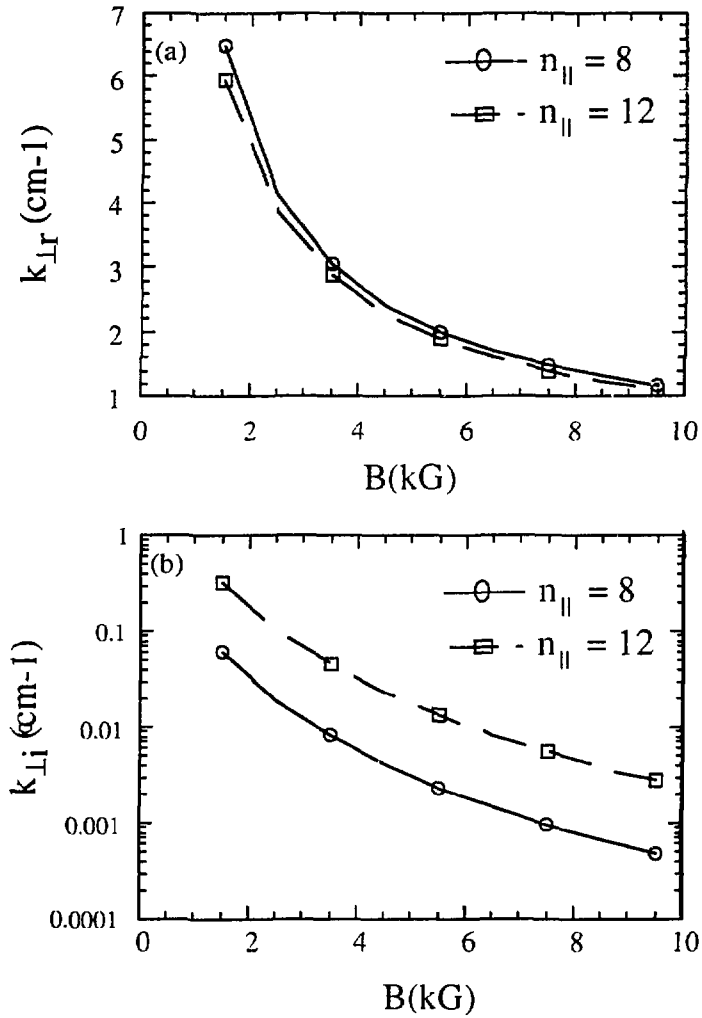

Fig. 2

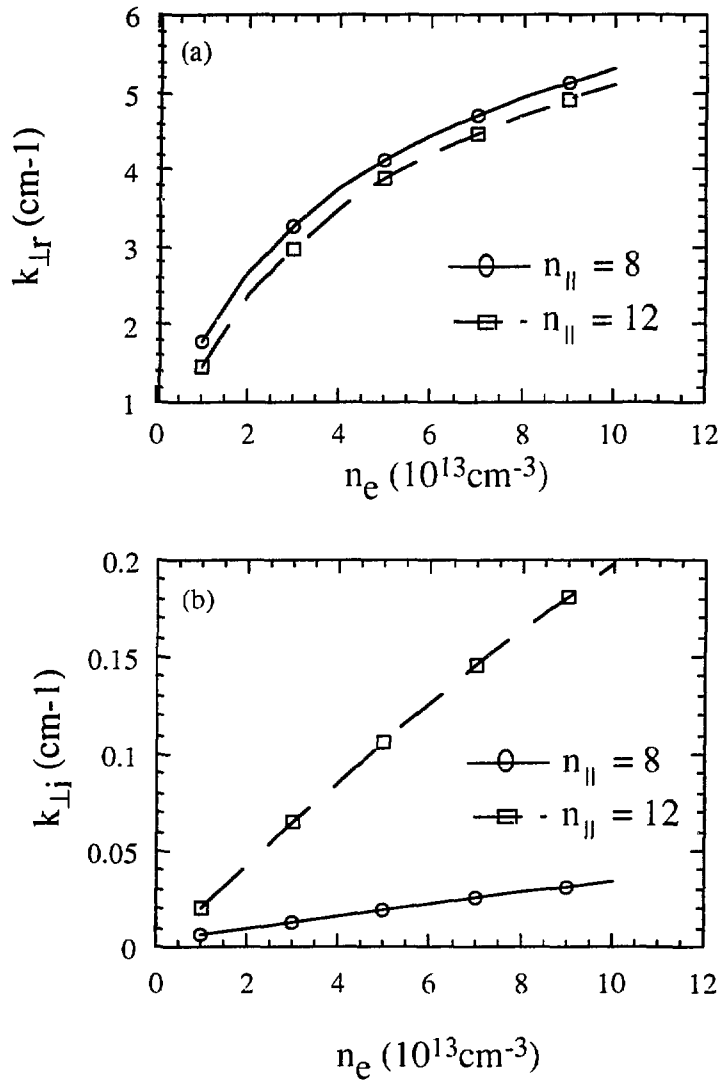

Fig. 3

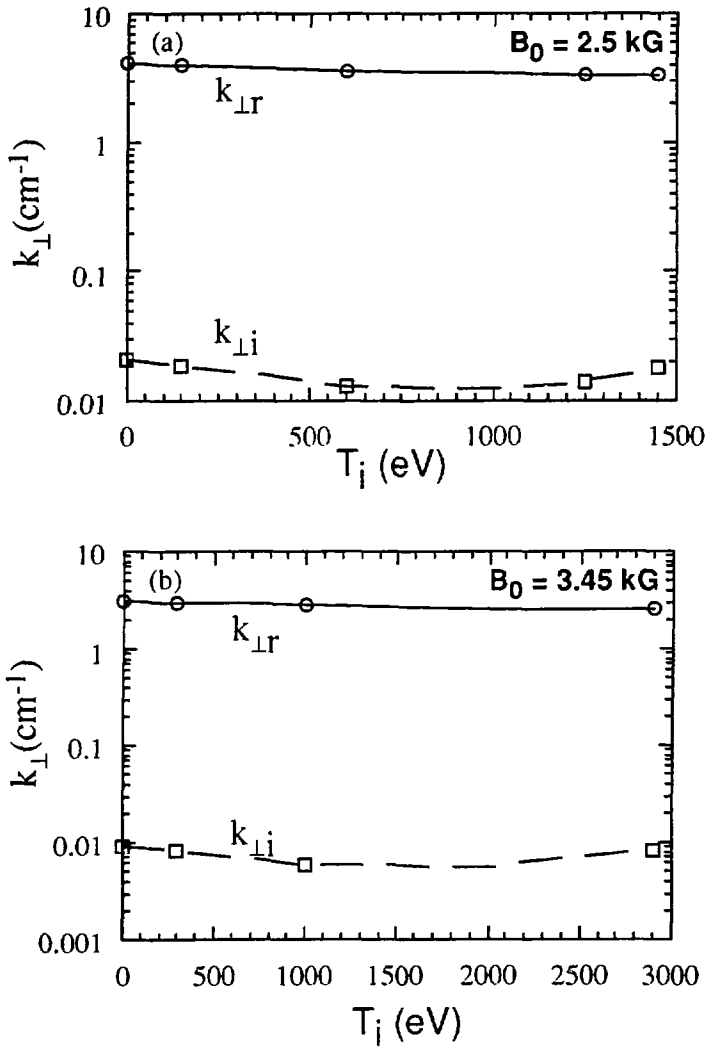
(a)
B_0 = 2.5 kG
$k_{\perp r}$
$k_{\perp i}$
$k_\perp$ (cm^{-1})
10
1
0.1
0.01
0
500
1000
1500
T_i (eV)
(b)
B_0 = 3.45 kG
$k_{\perp r}$
$k_{\perp i}$
$k_\perp$ (cm^{-1})
10
1
0.1
0.01
0.001
0
500
1000
1500
2000
2500
3000
T_i (eV)

Fig. 4

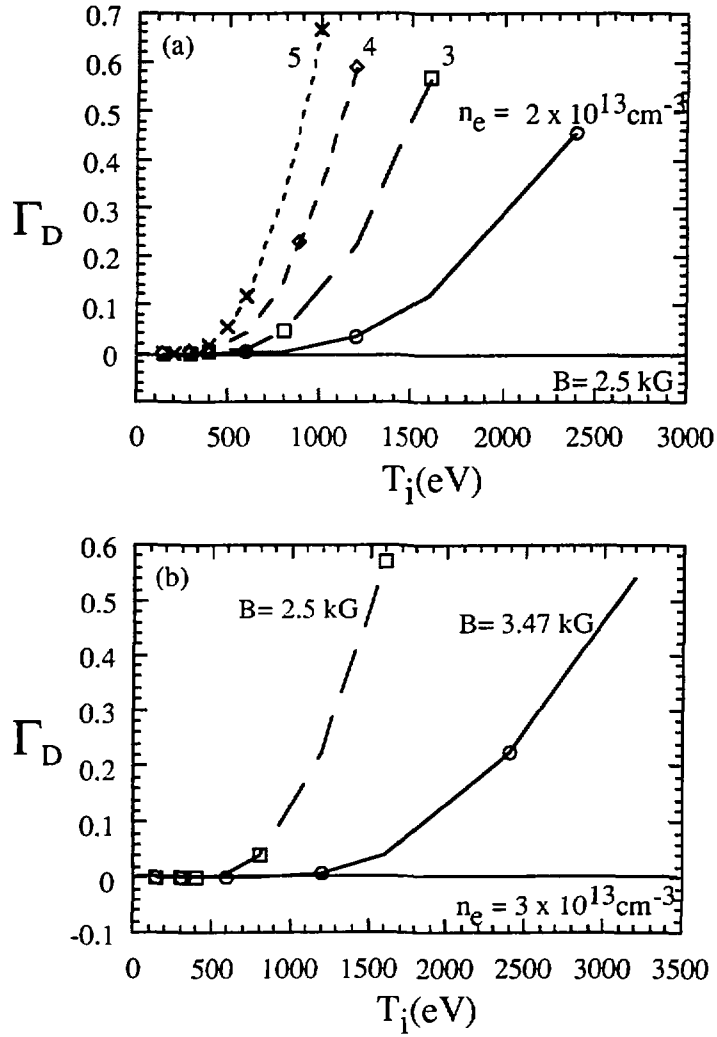
(a)
5
4
3
n_e = 2 x 10^{13}cm^{-3}
B= 2.5 kG
Γ_D
T_i(eV)
(b)
B= 2.5 kG
B= 3.47 kG
n_e = 3 x 10^{13}cm^{-3}
Γ_D
T_i(eV)

Fig. 5

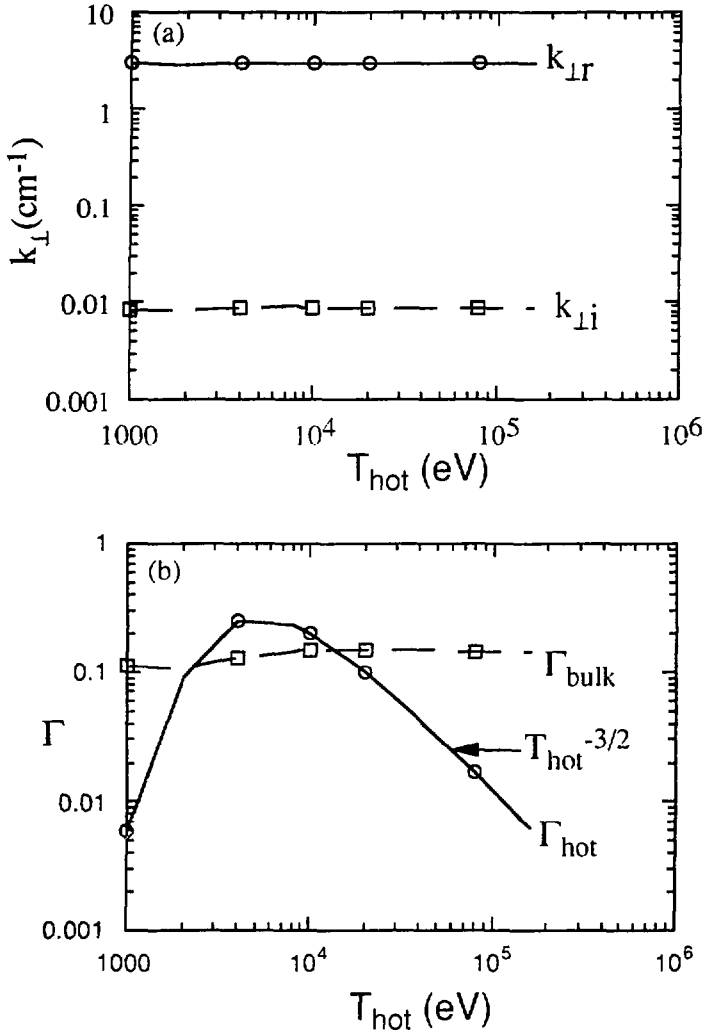
(a)
10
1
0.1
0.01
0.001
$k_\perp$ (cm^{-1})
$k_{\perp r}$
$k_{\perp i}$
1000
10^4
10^5
10^6
T_{hot} (eV)
(b)
1
0.1
0.01
0.001
Γ
Γ_{bulk}
$T_{hot}^{-3/2}$
Γ_{hot}
1000
10^4
10^5
10^6
T_{hot} (eV)

Fig. 6

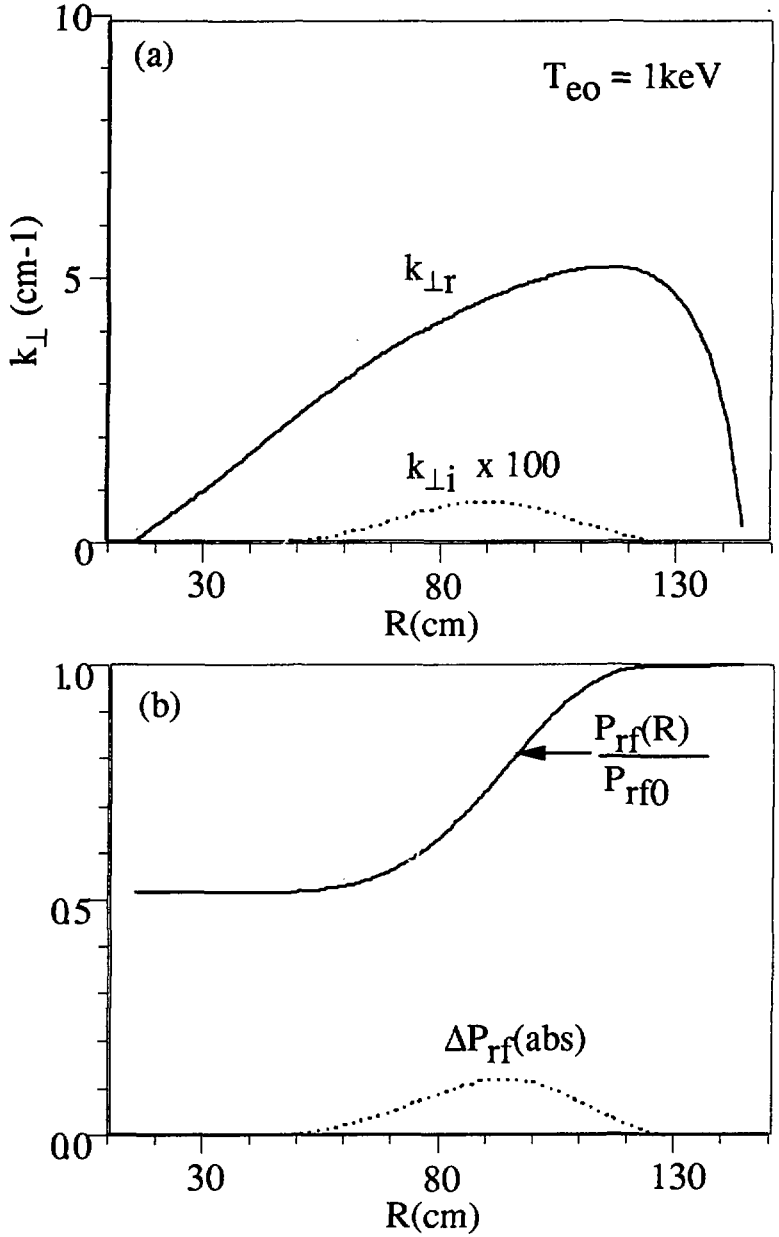
10
(a)
T_{eo} = 1keV
$k_{\perp r}$
5
$k_{\perp}$ (cm-1)
$k_{\perp i}$ x 100
0
30
80
130
R(cm)
1.0
(b)
$P_{rf}(R)$
P_{rf0}
0.5
ΔP_{rf}(abs)
0.0
30
80
130
R(cm)

Fig. 7

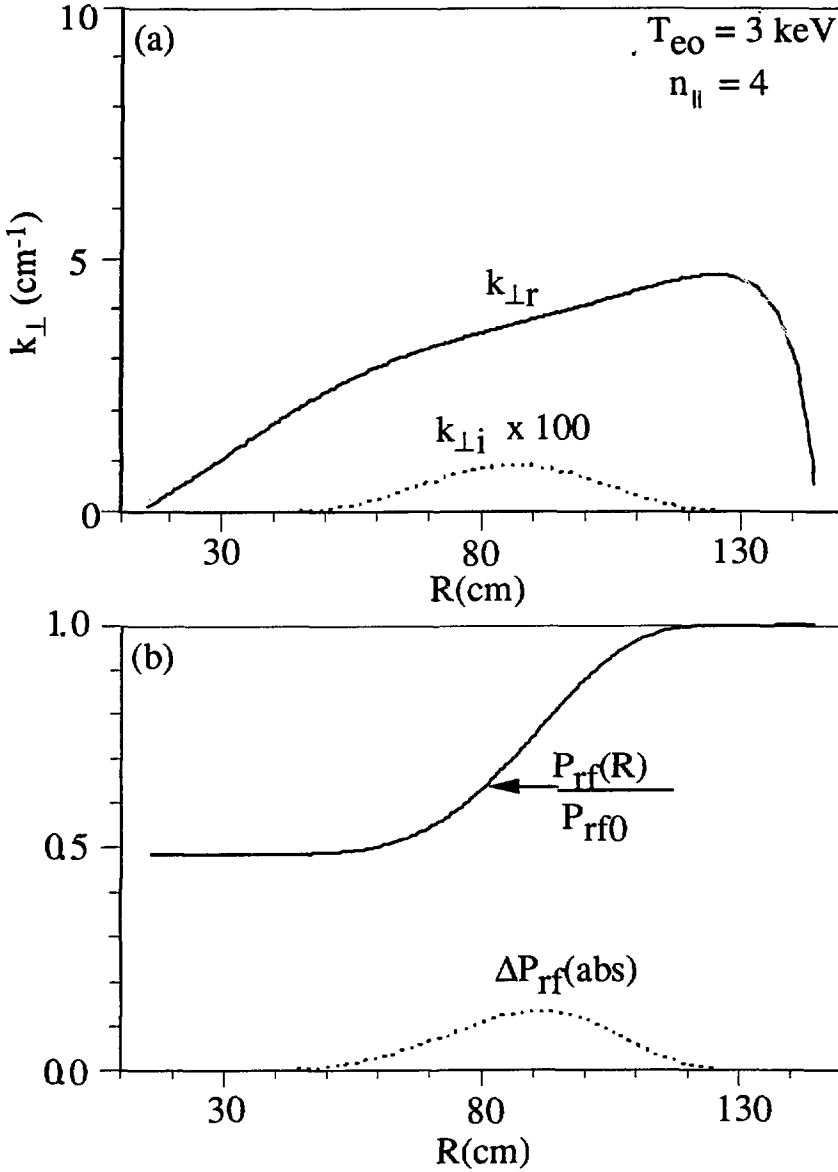
(a)
T_{eo} = 3 keV
$n_{||}$ = 4
$k_{\perp r}$
$k_{\perp i}$ x 100
$k_\perp$ (cm^{-1})
10
5
0
30
80
130
R(cm)
(b)
$P_{rf}(R)$
P_{rf0}
ΔP_{rf}(abs)
1.0
0.5
0.0
30
80
130
R(cm)

Fig. 8

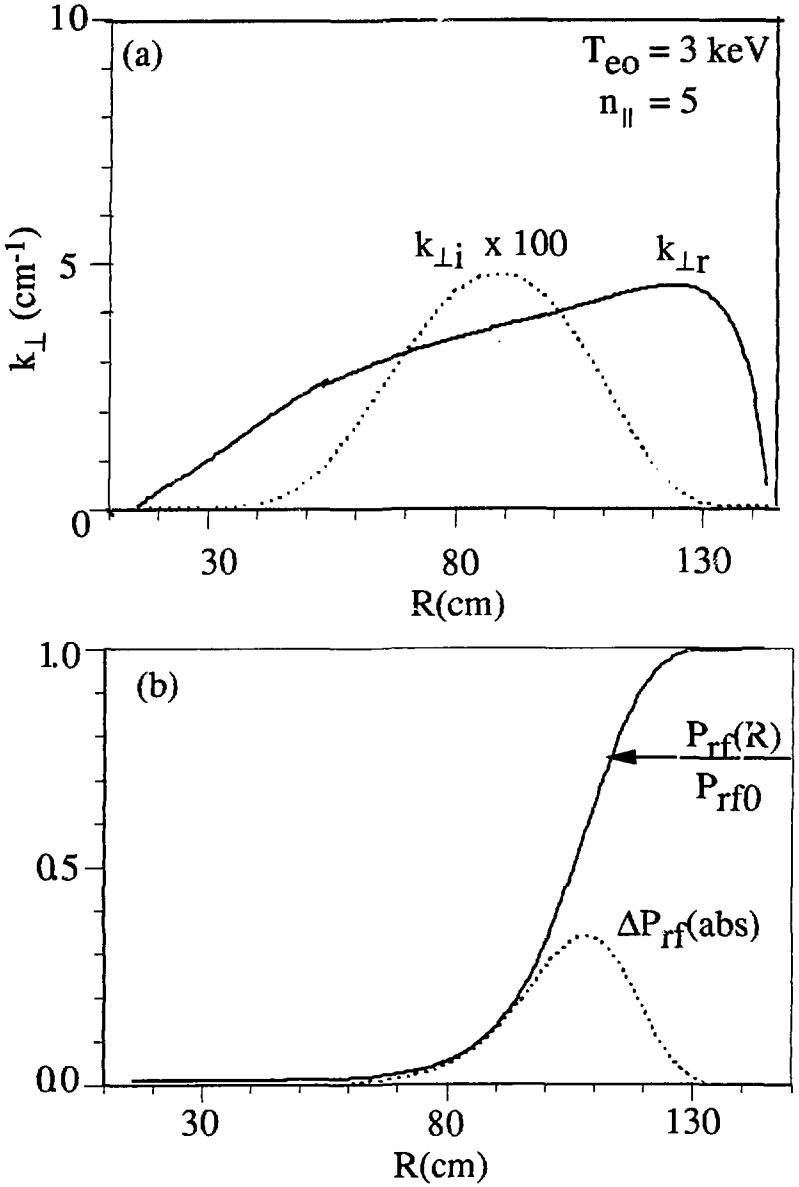
10
(a)
T_{eo} = 3 keV
$n_{\parallel}$ = 5
$k_{\perp i}$ x 100
$k_{\perp r}$
$k_{\perp}$ (cm^{-1})
5
0
30
80
130
R(cm)
1.0
(b)
$P_{rf}(R)$
P_{rf0}
ΔP_{rf}(abs)
0.5
0.0
30
80
130
R(cm)

Fig. 9

EXTERNAL DISTRIBUTION IN ADDITION TO UC-420

Dr. F. Paoloni, Univ. of Wollongong, AUSTRALIA
Prof. R.C. Cross, Univ. of Sydney, AUSTRALIA
Plasma Research Lab., Australian Nat. Univ., AUSTRALIA
Prof. I.R. Jones, Flinders Univ, AUSTRALIA
Prof. F. Cap, Inst. for Theoretical Physics, AUSTRIA
Prof. M. Heindler, Institut für Theoretische Physik, AUSTRIA
Prof. M. Goossens, Astronomisch Instituut, BELGIUM
Ecole Royale Militaire, Lab. de Phy. Plasmas, BELGIUM
Commission-European, DG. XII-Fusion Prog., BELGIUM
Prof. R. Boucique, Rijksuniversiteit Gent, BELGIUM
Dr. P.H. Sakanaka, Instituto Fisica, BRAZIL
Prof. Dr. I.C. Nascimento, Instituto Fisica, Sao Paulo, BRAZIL
Instituto Nacional De Pesquisas Espaciais-INPE, BRAZIL
Documents Office, Atomic Energy of Canada Ltd., CANADA
Ms. M. Morin, CCFM/Tokamak de Varennes, CANADA
Dr. M.P. Bachynski, MPB Technologies, Inc., CANADA
Dr. H.M. Skarsgard, Univ. of Saskatchewan, CANADA
Prof. J. Teichmann, Univ. of Montreal, CANADA
Prof. S.R. Sreenivasan, Univ. of Calgary, CANADA
Prof. R. Marchand, INRS-Energie et Materiaux, CANADA
Dr. R. Bolton, Centre canadien de fusion magnétique, CANADA
Dr. C.R. James,, Univ. of Alberta, CANADA
Dr. P. Lukác, Komenského Universzita, CZECHO-SLOVAKIA
The Librarian, Culham Laboratory, ENGLAND
Library, R61, Rutherford Appleton Laboratory, ENGLAND
Mrs. S.A. Hutchinson, JET Library, ENGLAND
Dr. S.C. Sharma, Univ. of South Pacific, FIJI ISLANDS
P. Mähönen, Univ. of Helsinki, FINLAND
Prof. M.N. Bussac, Ecole Polytechnique,, FRANCE
C. Mouttet, Lab. de Physique des Milieux Ionisés, FRANCE
J. Radet, CEN/CADARACHE - Bat 506, FRANCE
Prof. E. Economou, Univ. of Crete, GREECE
Ms. C. Rinni, Univ. of Ioannina, GREECE
Preprint Library, Hungarian Academy of Sci., HUNGARY
Dr. B. DasGupta, Saha Inst. of Nuclear Physics, INDIA
Dr. P. Kaw, Inst. for Plasma Research, INDIA
Dr. P. Rosenau, Israel Inst. of Technology, ISRAEL
Librarian, International Center for Theo Physics, ITALY
Miss C. De Palo, Associazione EURATOM-ENEA , ITALY
Dr. G. Grosso, Istituto di Fisica del Plasma, ITALY
Prof. G. Rostangni, Istituto Gas Ionizzati Del Cnr, ITALY
Dr. H. Yamato, Toshiba Res & Devel Center, JAPAN
Prof. I. Kawakami, Hiroshima Univ., JAPAN
Prof. K. Nishikawa, Hiroshima Univ., JAPAN
Librarian, Naka Fusion Research Establishment, JAERI, JAPAN
Director, Japan Atomic Energy Research Inst., JAPAN
Prof. S. Itoh, Kyushu Univ., JAPAN
Research Info. Ctr., National Instit. for Fusion Science, JAPAN
Prof. S. Tanaka, Kyoto Univ., JAPAN
Library, Kyoto Univ., JAPAN
Prof. N. Inoue, Univ. of Tokyo, JAPAN
Secretary, Plasma Section, Electrotechnical Lab., JAPAN
Dr. O. Mitarai, Kumamoto Inst. of Technology, JAPAN
Dr. G.S. Lee, Korea Basic Sci. Ctr., KOREA
J. Hyeon-Sook, Korea Atomic Energy Research Inst., KOREA
D.I. Choi, The Korea Adv. Inst. of Sci. & Tech., KOREA
Leandro Melendez Lugo, Inst. Nacl. de Inves. Nucl, MEXICO
Prof. B.S. Liley, Univ. of Waikato, NEW ZEALAND
inst of Physics, Chinese Acad Sci PEOPLE'S REP. OF CHINA
Library, Inst. of Plasma Physics, PEOPLE'S REP. OF CHINA
Tsinghua Univ. Library, PEOPLE'S REPUBLIC OF CHINA
Z. Li, S.W. Inst Physics, PEOPLE'S REPUBLIC OF CHINA
Prof. J.A.C. Cabral, Instituto Superior Tecnico, PORTUGAL
Prof. M.A. Hellberg, Univ. of Natal, S. AFRICA
Prof. D.E. Kim, Pohang Inst. of Sci. & Tech., SO. KOREA
Prof. C.I.E.M.A.T, Fusion Division Library, SPAIN
Dr. L. Stenflo, Univ. of UMEA, SWEDEN
Library, Royal Inst. of Technology, SWEDEN
Prof. H. Wilhelmson, Chalmers Univ. of Tech., SWEDEN
Centre Phys. Des Plasmas, Ecole Polytech, SWITZERLAND
Bibliotheek, Inst. Voor Plasma-Fysica, THE NETHERLANDS
Asst. Prof. Dr. S. Cakir, Middle East Tech. Univ., TURKEY
Dr. V.A. Glukhikh,Sci. Res. Inst. Electrophys.I Apparatus, USSR
Dr. D.D. Ryutov, Siberian Branch of Academy of Sci., USSR
Dr. G.A. Eliseev, I.V. Kurchatov Inst., USSR
Librarian, The Ukr.SSR Academy of Sciences, USSR
Dr. L.M. Kovrizhnykh, Inst. of General Physics, USSR
Kernforschungsanlage GmbH, Zentralbibliothek, W. GERMANY
Bibliothek, Inst. Für Plasmaforschung, W. GERMANY
Prof. K. Schindler, Ruhr-Universität Bochum, W. GERMANY
Dr. F. Wagner, (ASDEX), Max-Planck-Institut, W. GERMANY
Librarian, Max-Planck-Institut, W. GERMANY